Relations between scattering data and material parameters in complex media

Friden, Jonas

1995

CODEN:LUTEDX/(TEAT-7038)/1-12/(1995)

Relations between scattering data and material parameters in complex media

Jonas Fridén

Electromagnetic Theory
Department of Electrical and Information Technology
Lund University
Sweden

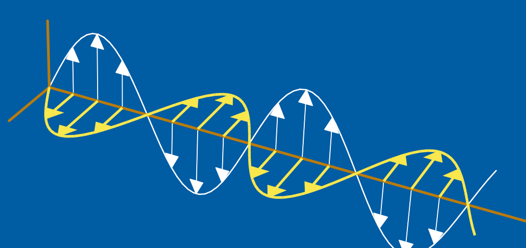

(TEAT-7038)/1-12/(1995): J. Fridén, Relations between scattering data and material parameters in complex media

Jonas Fridén

Institute of Theoretical Physics
Chalmers University of Technology
University of Göteborg
SE-412 96 Göteborg
Sweden

Editor: Gerhard Kristensson

CODEN:LUTEDX/(TEAT-7038)/1-12/(1995)

Relations between scattering data and material parameters in complex media

Jonas Fridén

Electromagnetic Theory
Department of Electrical and Information Technology
Lund University
Sweden

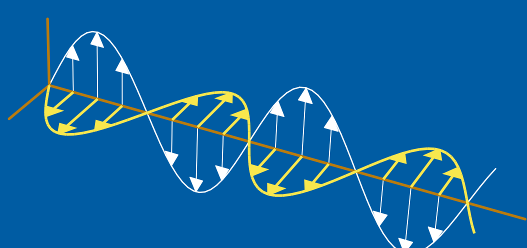

Jonas Fridén

Institute of Theoretical Physics
Chalmers University of Technology
University of Göteborg
SE-412 96 Göteborg
Sweden

Editor: Gerhard Kristensson

Abstract

The symmetries of scattering data of a bianisotropic, homogeneous and dispersive slab are investigated. It is demonstrated how these symmetries can be used to reveal the symmetries of the medium parameters (four three-dimensional susceptibility kernels). The underlying physical experiment is a transient electromagnetic plane wave obliquely incident upon the slab. The analysis is based on time-domain techniques and a wave splitting transformation. The results follow from the assumed unique solubility of an inverse problem for the split fields used earlier in the anisotropic case. The building blocks in the method presented here is a set of transformations between mirror image pair experiments. The main symmetry classes that can be detected using this method are the spatial-reversal symmetric (anisotropic) and the transversely or longitudinally mirror image symmetric media. More symmetric classes are the bianisotropic axially symmetric and the mirror image symmetric media.

1 Introduction

In a series of earlier studies the direct and the inverse medium scattering problems for a slab containing a homogeneous complex medium are considered [1–4, 7, 8, 12]. These problems are solved using time-domain techniques (wave-splitting and imbedding or a Green functions technique) and the medium is assumed to be bi-isotropic, gyrotropic or anisotropic. In Ref. [3] an algorithm for the inverse problem in the anisotropic case is presented. The generalization from the ansiotropic to the bianisotropic case is straightforward and the same method applies (slightly generalized). Therefore, in this paper, the solution of the inverse problem is not addressed. However, the symmetry properties of the scattering data can be used to detect the symmetry properties of the medium. This is the main result of this paper and it is based on the ideas and results in Ref. [3].

To put the present work in its context, the background is briefly described. The basic equations for the electromagnetic fields are the Maxwell equations and the constitutive relations. These equations can be cast in a two-dimensional form via an elimination of the field components normal to the plane of the slab. A change of indepenedent variables (or fields) then leads to an equation for the split (left- and right-going) fields. The dynamics inverse problem (DIP) is to recover the coefficients in this particular equation (the dynamics). In Ref. [3] it is demonstrated how to solve the DIP by using complete scattering data from a mirror image pair (MIP). Each MIP comprises two experiments with incident directions that are mutually mirror images in the plane of the slab. Furthermore, if the coefficients in the dynamics are known the coefficients in the equation for the parallel fields is known, see Ref. [3]. The paralell fields are the components of the electric and the magnetic fields ($\boldsymbol{E}$ and $\boldsymbol{H}$) parallel to the boundaries of the slab. In the equation for the parallel fields the coefficients are four two-dimensional dyadics $\mathbf{D}_{\kappa\lambda}$. To retrieve the susceptibility dyadics (the coefficients in the constitutive relations) from these coefficients several MIPs are needed, cf. Ref. [3].

In this paper unique solubility of the DIP is assumed, i.e., for any MIP the dyadics $\mathbf{D}_{\kappa\lambda}$ are known. These coefficients are derived in Section 2. In Section 3 a method to distinguish different types of bianisotropic media is given. This method uses three basic transformations of a MIP, two mirror images (longitudinal and transverse) and a rotation around the normal of the slab. Combination of the mirror images yields the spatial reversal transformation that, as demonstrated, can be used to select the anisotropic media. Note, only a finite number of experiments is needed and the full inverse problem for these experiments does not have to be solved, i.e., the exact functional form of the susceptibility dyadics are not needed. Merely the symmetry of the scattering data is used.

2 Basic equations

Consider an electromagnetic plane wave incident, along the unit vector $\hat{\boldsymbol{k}}$, on a slab of homogeneous, dispersive and bianisotropic medium. Interactions between the electromagnetic fields and the medium in the slab are modelled with the constitutive relations. The constitutive relations for a bianisotropic medium with no optical response, see Ref. [6], can be written in the form[1,2]

$$\begin{aligned} \boldsymbol{D} &= \epsilon_0(\boldsymbol{E} + \boldsymbol{\chi}_{ee} * \boldsymbol{E} + \boldsymbol{\chi}_{em} * \eta_0 \boldsymbol{H}), \\ \eta_0 \boldsymbol{B} &= \mu_0(\eta_0 \boldsymbol{H} + \boldsymbol{\chi}_{me} * \boldsymbol{E} + \boldsymbol{\chi}_{mm} * \eta_0 \boldsymbol{H}). \end{aligned} \tag{2.1}$$

Here ϵ_0, μ_0 and η_0 are the permittivity, permeability and the wave impedance of vacuum, respectively. In anisotropic media there is no microscopic coupling between the electric and the magnetic fields. Therefore, anisotropic media are characterized by

$$\boldsymbol{\chi}_{em} \equiv \boldsymbol{\chi}_{me} \equiv \mathbf{0}. \tag{2.2}$$

If in addition the medium is reciprocal the kernels $\boldsymbol{\chi}_{\kappa\kappa}$, $\kappa = e,\ m$, are symmetric. Another important class is the bi-isotropic media wherein the susceptibility dyadics have the form

$$\boldsymbol{\chi}_{\kappa\lambda} = \chi_{\kappa\lambda}\mathbf{I}, \quad \kappa, \lambda = e, m, \tag{2.3}$$

where $\mathbf{I}$ is the three-dimensional unit dyadic.

Introduce a unit vector $\hat{\boldsymbol{n}}$ normal to the slab and decompose $\hat{\boldsymbol{k}}$ in a normal and a parallel component ($\hat{\boldsymbol{k}} = \boldsymbol{k}_\parallel + k_n \hat{\boldsymbol{n}}$). Due to the plane wave form of the excitation, the fields inside the slab vary only with $n = \boldsymbol{r} \cdot \hat{\boldsymbol{n}}$ and $s = t - \boldsymbol{r} \cdot \boldsymbol{k}_\parallel / c_0$, where c_0 is the phase velocity of vacuum.

The equation for the parallel fields is derived for anisotropic media in Refs [2–4]. The same method can be used for bianisotropic media. Use the Maxwell equations, the constitutive relations and the decomposition

[1] The symbol $*$ denotes causal time convolution.

[2] With this notation all susceptibility dyadics $\boldsymbol{\chi}_{\kappa\lambda}$ have the same dimension (inverse time).

$$\begin{aligned}&\boldsymbol{E} = \boldsymbol{E}_\parallel + E_n\hat{\boldsymbol{n}}, \quad \boldsymbol{H} = \boldsymbol{H}_\parallel + H_n\hat{\boldsymbol{n}},\\ &\mathbf{I} = \mathbf{I}_\parallel + \hat{\boldsymbol{n}}\hat{\boldsymbol{n}},\\ &\boldsymbol{\chi}_{\kappa\lambda} = \boldsymbol{\chi}_{\parallel,\kappa\lambda} + \hat{\boldsymbol{n}}\boldsymbol{a}_{\kappa\lambda} + \boldsymbol{b}_{\kappa\lambda}\hat{\boldsymbol{n}} + \hat{\boldsymbol{n}}c_{\kappa\lambda}\hat{\boldsymbol{n}}, \quad \kappa,\, \lambda = e,\, m,\end{aligned} \tag{2.4}$$

for vectors and dyadics, respectively. By use of the resolvent equation

$$L_{\kappa\lambda} + c_{\kappa\lambda} + \sum_{\nu=e,m} L_{\kappa\nu} * c_{\nu\lambda} = 0 \tag{2.5}$$

the normal field components E_n and H_n are eliminated and the equation for the parallel fields takes the form[3]

$$\begin{aligned}c_0\partial_n \begin{pmatrix} \boldsymbol{E}_\parallel \\ \hat{\boldsymbol{n}} \times \eta_0\boldsymbol{H}_\parallel \end{pmatrix} = &\begin{pmatrix} \mathbf{0} & \mathbf{I}_\parallel - \boldsymbol{k}_\parallel\boldsymbol{k}_\parallel \\ \mathbf{I}_\parallel - (\boldsymbol{k}_\parallel \times \hat{\boldsymbol{n}})(\boldsymbol{k}_\parallel \times \hat{\boldsymbol{n}}) & \mathbf{0} \end{pmatrix} \partial_s \begin{pmatrix} \boldsymbol{E}_\parallel \\ \hat{\boldsymbol{n}} \times \eta_0\boldsymbol{H}_\parallel \end{pmatrix}\\ &+ \begin{pmatrix} \mathbf{D}_{ee} & \mathbf{D}_{em} \\ \mathbf{D}_{me} & \mathbf{D}_{mm} \end{pmatrix} * \partial_s \begin{pmatrix} \boldsymbol{E}_\parallel \\ \hat{\boldsymbol{n}} \times \eta_0\boldsymbol{H}_\parallel \end{pmatrix}.\end{aligned} \tag{2.6}$$

To see the structure of $\mathbf{D}_{\kappa\lambda}$, decompose using the notation

$$\mathbf{D}_{\kappa\lambda} = \mathbf{D}_{\kappa\lambda}^{(0)} + \mathbf{D}_{\kappa\lambda}^{(1)} + \mathbf{D}_{\kappa\lambda}^{(2)}. \tag{2.7}$$

Here $\mathbf{D}_{\kappa\lambda}^{(0)}$ does not depend on $\boldsymbol{k}_\parallel$ whereas $\mathbf{D}_{\kappa\lambda}^{(1,2)}$ contain first and second order dyads in $\boldsymbol{k}_\parallel$, respectively. Straightforward but lengthy calculations show that the dyadics $\mathbf{D}_{\kappa\lambda}^{(i)}$ for $\kappa,\ \lambda = e, m$ and $i = 0, 1, 2$ are

$$\begin{aligned}\mathbf{D}_{ee}^{(0)} =&\hat{\boldsymbol{n}} \times \boldsymbol{\chi}_{\parallel,me} - (\hat{\boldsymbol{n}} \times \boldsymbol{b}_{me}) * [(1 + L_{ee}*)\boldsymbol{a}_{ee} + L_{em} * \boldsymbol{a}_{me}]\\ &- (\hat{\boldsymbol{n}} \times \boldsymbol{b}_{mm}) * [L_{me} * \boldsymbol{a}_{ee} + (1 + L_{mm}*)\boldsymbol{a}_{me}],\end{aligned} \tag{2.8}$$

$$\begin{aligned}\mathbf{D}_{ee}^{(1)} =&(1 + L_{ee}*)\boldsymbol{k}_\parallel\boldsymbol{a}_{ee} + L_{em} * \boldsymbol{k}_\parallel\boldsymbol{a}_{me}\\ &+ (\hat{\boldsymbol{n}} \times \boldsymbol{b}_{me})(\hat{\boldsymbol{n}} \times \boldsymbol{k}_\parallel) * L_{em} + (\hat{\boldsymbol{n}} \times \boldsymbol{b}_{mm})(\hat{\boldsymbol{n}} \times \boldsymbol{k}_\parallel)(1 + *L_{mm}),\end{aligned} \tag{2.9}$$

$$\mathbf{D}_{ee}^{(2)} = - \boldsymbol{k}_\parallel(\hat{\boldsymbol{n}} \times \boldsymbol{k}_\parallel)L_{em}, \tag{2.10}$$

$$\begin{aligned}\mathbf{D}_{em}^{(0)} =& - \hat{\boldsymbol{n}} \times \boldsymbol{\chi}_{\parallel,mm} \times \hat{\boldsymbol{n}} - (\hat{\boldsymbol{n}} \times \boldsymbol{b}_{me}) * [(1 + L_{ee}*)(\hat{\boldsymbol{n}} \times \boldsymbol{a}_{em}) + L_{em} * (\hat{\boldsymbol{n}} \times \boldsymbol{a}_{mm})]\\ &- (\hat{\boldsymbol{n}} \times \boldsymbol{b}_{mm}) * [L_{me} * (\hat{\boldsymbol{n}} \times \boldsymbol{a}_{em}) + (1 + L_{mm}*)(\hat{\boldsymbol{n}} \times \boldsymbol{a}_{mm})],\end{aligned} \tag{2.11}$$

$$\begin{aligned}\mathbf{D}_{em}^{(1)} =&(1 + L_{ee}*)\boldsymbol{k}_\parallel(\hat{\boldsymbol{n}} \times \boldsymbol{a}_{em}) + L_{em} * \boldsymbol{k}_\parallel(\hat{\boldsymbol{n}} \times \boldsymbol{a}_{mm})\\ &+ (\hat{\boldsymbol{n}} \times \boldsymbol{b}_{me})\boldsymbol{k}_\parallel(1 + *L_{ee}) + (\hat{\boldsymbol{n}} \times \boldsymbol{b}_{mm})\boldsymbol{k}_\parallel * L_{me},\end{aligned} \tag{2.12}$$

$$\mathbf{D}_{em}^{(2)} = - \boldsymbol{k}_\parallel\boldsymbol{k}_\parallel L_{ee}, \tag{2.13}$$

[3] In the following, all dyadics are two-dimensional and normal to $\hat{\boldsymbol{n}}$, i.e., $\hat{\boldsymbol{n}} \cdot \mathbf{A} = \mathbf{A} \cdot \hat{\boldsymbol{n}} = \mathbf{0}$.

$$\begin{aligned}\mathbf{D}_{me}^{(0)} =&\boldsymbol{\chi}_{\parallel,ee} - \boldsymbol{b}_{ee} * [(1 + L_{ee}*)\boldsymbol{a}_{ee} + L_{em} * \boldsymbol{a}_{me}]\\ &- \boldsymbol{b}_{em} * [L_{me} * \boldsymbol{a}_{ee} + (1 + L_{mm}*)\boldsymbol{a}_{me}], \end{aligned} \tag{2.14}$$

$$\begin{aligned}\mathbf{D}_{me}^{(1)} =&L_{me} * (\hat{\boldsymbol{n}} \times \boldsymbol{k}_\parallel)\boldsymbol{a}_{ee} + (1 + L_{mm}*)(\hat{\boldsymbol{n}} \times \boldsymbol{k}_\parallel)\boldsymbol{a}_{me}\\ &+ \boldsymbol{b}_{ee}(\hat{\boldsymbol{n}} \times \boldsymbol{k}_\parallel) * L_{em} + \boldsymbol{b}_{em}(\hat{\boldsymbol{n}} \times \boldsymbol{k}_\parallel)(1 + *L_{mm}),\end{aligned} \tag{2.15}$$

$$\mathbf{D}_{me}^{(2)} = - (\hat{\boldsymbol{n}} \times \boldsymbol{k}_\parallel)(\hat{\boldsymbol{n}} \times \boldsymbol{k}_\parallel)L_{mm}, \tag{2.16}$$

$$\begin{aligned}\mathbf{D}_{mm}^{(0)} =& - \boldsymbol{\chi}_{\parallel,em} \times \hat{\boldsymbol{n}} - \boldsymbol{b}_{ee} * [(1 + L_{ee}*)(\hat{\boldsymbol{n}} \times \boldsymbol{a}_{em}) + L_{em} * (\hat{\boldsymbol{n}} \times \boldsymbol{a}_{mm})]\\ &- \boldsymbol{b}_{em} * [L_{me} * (\hat{\boldsymbol{n}} \times \boldsymbol{a}_{em}) + (1 + L_{mm}*)(\hat{\boldsymbol{n}} \times \boldsymbol{a}_{mm})],\end{aligned} \tag{2.17}$$

$$\begin{aligned}\mathbf{D}_{mm}^{(1)} =&L_{me} * (\hat{\boldsymbol{n}} \times \boldsymbol{k}_\parallel)(\hat{\boldsymbol{n}} \times \boldsymbol{a}_{em}) + (1 + L_{mm}*)(\hat{\boldsymbol{n}} \times \boldsymbol{k}_\parallel)(\hat{\boldsymbol{n}} \times \boldsymbol{a}_{mm})\\ &+ \boldsymbol{b}_{ee}\boldsymbol{k}_\parallel * (1 + *L_{ee}) + \boldsymbol{b}_{em}\boldsymbol{k}_\parallel * L_{me},\end{aligned} \tag{2.18}$$

$$\mathbf{D}_{mm}^{(2)} = - (\hat{\boldsymbol{n}} \times \boldsymbol{k}_\parallel)\boldsymbol{k}_\parallel L_{me}. \tag{2.19}$$

It is straightforward to see that the dyadics in Eqs (2.8), ..., (2.19) have the following generic representation

$$\mathbf{J}^{\delta_{\kappa m}} \cdot \mathbf{D}_{\kappa\lambda} \cdot \mathbf{J}^{\delta_{\lambda e}}(\boldsymbol{k}_\parallel) = \boldsymbol{\alpha}_{\kappa\lambda} + \boldsymbol{k}_\parallel\boldsymbol{\beta}_{R,\kappa\lambda} + \boldsymbol{\beta}_{L,\kappa\lambda}\boldsymbol{k}_\parallel + \gamma_{\kappa\lambda}\boldsymbol{k}_\parallel\boldsymbol{k}_\parallel, \tag{2.20}$$

see also Appendix A. Here $\delta_{\kappa\lambda}$ is the Kronecker symbol, $\mathbf{J} = \hat{\boldsymbol{n}} \times \mathbf{I}_\parallel$, $\boldsymbol{\alpha}_{\kappa\lambda}$ are two-dimensional dyadics, $\boldsymbol{\beta}_{R/L,\kappa\lambda}$ are two-dimensional vectors and $\gamma_{\kappa\lambda}$ are scalars.

From Eq. (2.6) it is straightforward to do a wave splitting transformation and to derive the equations for the reflection and transmission kernels for a Mirror Image Pair (MIP) [3].

3 Symmetries

The objective of this section is to outline the connection between the symmetries of the scattering data and the material parameters. This is done by studying transformations between scattering experiments. To continue, some definitions and results from Ref. [3] are needed.

The MIP (mirror image pair) and the corresponding scattering data are basic building blocks. Roughly speaking, the scattering data of the MIP comprises the wave front propagators and the reflection- and transmission-kernels of the incident directions in the MIP, i.e., $\hat{\boldsymbol{k}} = \boldsymbol{k}_\parallel \pm k_n\hat{\boldsymbol{n}}$. Furthermore, the slab is assumed to be sufficiently thin so that the wave front is rotated less than a half turn. This constraint is crucial for the non-reciprocal or the non-anisotropic media [3, 6]. With this constraint, on the thickness of the slab, the results in Ref. [3] indicate that the complete scattering data uniquely determine $\mathbf{D}_{\kappa\lambda}$, i.e., the DIP (dynamics inverse problem) has a unique solution. For further details on the MIP and the DIP see Ref. [3].

To study the relation between the symmetry of the scattering data and the susceptibility kernels it is relevant to study the transformations depicted in Fig. 1.

By inspection of the results in Ref. [3] and Eqs (2.8), . . ., (2.19) it is straightforward to obtain the corresponding transformation rules for $\mathbf{D}_{\kappa\lambda}^{(i)}$. The mirror image

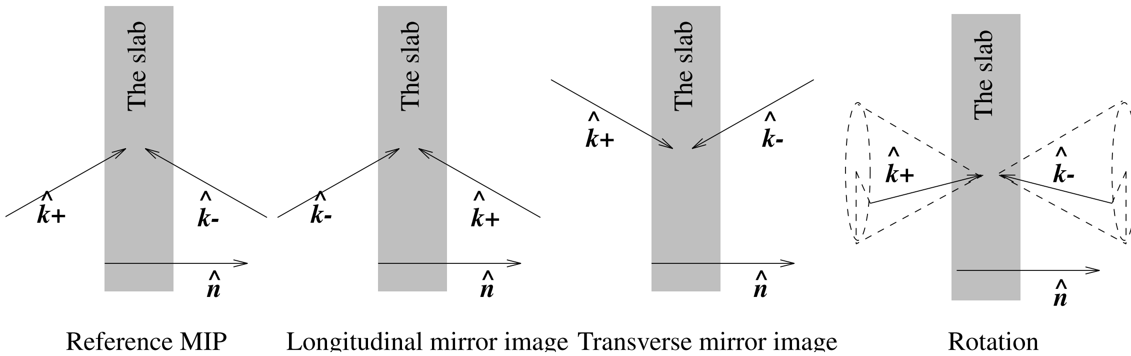

Figure 1: Basic $|k_n|$-preserving transformations of a MIP. Here $\hat{\boldsymbol{k}}\pm = \boldsymbol{k}_\parallel \pm |k_n|$ in the reference MIP.

transformations are either an identity or a change of sign in each $\mathbf{D}_{\kappa\lambda}^{(i)}$-dyadic. Thus the parity of $\mathbf{D}_{\kappa\lambda}^{(i)}$ due to the longitudinal and transverse mirror images, denoted $\mathcal{P}_t$ and $\mathcal{P}_l$, is defined. These quantities are

$$\mathcal{P}_l = (-1)^{\delta_{\kappa\lambda}}, \qquad \mathcal{P}_t = (-1)^i. \tag{3.1}$$

Furthermore, for the rotation to be distinct from the transverse mirror image the angle of rotation is restricted to belong to the open interval $(0, \pi)$.

To solve the full inverse problem or to obtain the symmetry results of this section several MIPs are needed. The choice of MIPs are due to

1. *Each MIP (fixed* $\boldsymbol{k}_\parallel$*) uniquely determines* $\mathbf{D}_{\kappa\lambda}(\boldsymbol{k}_\parallel)$*, [3],*

2. *The set of MIPs must be complete, Appendix A.*

The first statement assumes unique solubility of the DIP and the condition for the completeness of the set of incident directions is derived in Appendix A. Explicitly, it reads

$$\hat{\boldsymbol{n}} \cdot [(\boldsymbol{k}_\parallel^{(1)} - \boldsymbol{k}_\parallel^{(3)}) \times (\boldsymbol{k}_\parallel^{(2)} - \boldsymbol{k}_\parallel^{(3)})] \neq 0. \tag{3.2}$$

3.1 Anisotropic media

On a microscopic level anisotropic media are symmetric under temporal reversal or spatial reversal, cf. Ref. [9, 11] or Section 4. This is not the case in general if $\boldsymbol{\chi}_{em}$ and $\boldsymbol{\chi}_{me}$ are non-zero. Therefore to detect anisotropy one should use spatial reversal symmetry.

The spatial reversal transformation of a MIP is obtained by performing the transverse and longitudinal mirror images consecutively. The parity, cf. Eq. (3.1), of the $\mathbf{D}_{\kappa\lambda}^{(i)}$ dyadics therefore is

$$\mathcal{P}_{sr} = \mathcal{P}_l\mathcal{P}_t = (-1)^{\delta_{\kappa\lambda}+i}.$$

The relevant set of incident directions needed here comprises the MIPs and their spatial reversals corresponding to *two* non-parallel $\boldsymbol{k}_\parallel$s. Thus the set consists of four MIPs which form a complete set. This is so since any three MIPs in the set satisfy the completeness condition (3.2). Furthermore, this set is the smallest complete set that contain all incident directions with relevant scattering data, i.e., for any incident direction the spatially reversed direction is also included.

If the scattering data in this set of MIPs is spatial reversal symmetric and the DIP has a unique solution, the following holds for each MIP[4]:

$$\mathbf{D}^{(0)}_{\kappa\kappa}(\boldsymbol{k}_\parallel) + \mathbf{D}^{(2)}_{\kappa\kappa}(\boldsymbol{k}_\parallel) \equiv \mathbf{D}^{(1)}_{\kappa\overline{\kappa}}(\boldsymbol{k}_\parallel) \equiv \mathbf{0}.$$

Completeness, see Appendix A, then implies

$$\boldsymbol{\alpha}_{\kappa\kappa} \equiv \mathbf{0}, \quad \gamma_{\kappa\kappa} \equiv 0, \quad \boldsymbol{\beta}_{R/L,\kappa\overline{\kappa}} \equiv \mathbf{0}.$$

These identities use the notation of Eq. (2.20). Hence, by Eqs (2.10) and (2.19) $L_{\kappa\overline{\kappa}} \equiv 0$. The unique solubility of the Volterra equation (2.5) then implies $c_{\kappa\overline{\kappa}} \equiv 0$ [10]. Now use $L_{\kappa\overline{\kappa}} \equiv 0$ in Eqs (2.12) and (2.15). Again, the unique solubility of the resolvent equation is used to conclude

$$\boldsymbol{a}_{\kappa\overline{\kappa}} \equiv \boldsymbol{b}_{\kappa\overline{\kappa}} \equiv \mathbf{0}.$$

From Eqs (2.8) and (2.17) it follows that also $\boldsymbol{\chi}_{\parallel,\kappa\overline{\kappa}}$ must vanish identically. This implies that the entire dyadics $\boldsymbol{\chi}_{\kappa\overline{\kappa}}$ vanish identically and the medium is anisotropic.

Conclusion 1. *If the scattering data, for two MIPs with non-parallel $\boldsymbol{k}_\parallel$, are spatial reversal symmetric then the medium is anisotropic.*

Note, the incident directions with indpendent scattering data is exactly what is needed to solve the inverse problem for the homogeneous anisotropic slab, see Ref. [3].

3.2 Transversely mirror image symmetric media

Now study the transverse mirror image transformation, i.e., $\boldsymbol{k}_\parallel \to -\boldsymbol{k}_\parallel$. The relevant set of incident directions is generated by this operation acting on the MIPs corresponding to *two* non-parallel $\boldsymbol{k}_\parallel$s. The resulting set therefore comprises a complete set of incident directions, cf. Eq.(3.2), and all transverse mirror images are included in the set.

If the scattering data is transversely mirror image symmetric for the incident directions of this set Eq. (3.1) implies $\mathbf{D}^{(1)}_{\kappa\lambda}(\boldsymbol{k}_\parallel) = \mathbf{0}$, i.e., the dyadics with $\mathcal{P}_t = -1$ vanish. The completeness of the set (Appendix A) then uniquely determines all $\boldsymbol{\alpha}_{\kappa\lambda}$, $\boldsymbol{\beta}_{R/L,\kappa\lambda}$ and $\gamma_{\kappa\lambda}$ of $\mathbf{D}_{\kappa\lambda}$. This implies that

$$\boldsymbol{\beta}_{R/L,\kappa\lambda} \equiv \mathbf{0}.$$

[4]The notation of dual indices defined by $\overline{e} = m$ and $\overline{m} = e$ is used.

since $\mathbf{D}^{(1)}_{\kappa\lambda}(\boldsymbol{k}_\parallel) \equiv \mathbf{0}$. By inspection of Eqs (2.9), (2.12), (2.15) and (2.18) the vanishing of $\boldsymbol{\beta}_{R,\kappa\lambda}$ implies

$$\sum_{\nu=e,m} (\delta_{\kappa\nu} + L_{\kappa\nu}*)\boldsymbol{a}_{\nu\lambda} = \mathbf{0}, \qquad \kappa,\lambda = e,m,$$

and analogously for $\boldsymbol{\beta}_{L,\kappa\lambda}$

$$\sum_{\nu=e,m} \boldsymbol{b}_{\kappa\nu}(\delta_{\nu\lambda} + *L_{\nu\lambda}) = \mathbf{0}, \qquad \kappa,\lambda = e,m.$$

The unique solution of the Volterra equation (2.5) then implies that all the vectors $\boldsymbol{a}_{\kappa\lambda}$ and $\boldsymbol{b}_{\kappa\lambda}$ vanish identically.

Conclusion 2. *If the scattering data, for two MIPs with non-parallel $\boldsymbol{k}_\parallel$, are transversely mirror image symmetric then the susceptibility dyadics $\boldsymbol{\chi}_{\kappa\lambda}$ have the form $\boldsymbol{\chi}_{\kappa\lambda} = \boldsymbol{\chi}_{\parallel,\kappa\lambda} + \hat{\boldsymbol{n}}\hat{\boldsymbol{n}}c_{\kappa\lambda}$.*

3.3 Longitudinally mirror image symmetric media

The next transformation is the longitudinal mirror image, i.e., $k_n \to -k_n$. This transformation applied to a MIP is an identity and therefore it suffices to consider *three* MIPs with $\boldsymbol{k}_\parallel$s satisfying Eq. (3.2).

If the scattering data for these MIPs is longitudinally mirror image symmetric the dyadics $\mathbf{D}^{(i)}_{\kappa\kappa}(\boldsymbol{k}_\parallel)$ ($\mathcal{P}_l = -1$) vanish identically, cf. Eq. (3.1). Use of the completeness of the incident directions, see Appendix A, and the notation of Eq. (2.20) then yields

$$\boldsymbol{\alpha}_{\kappa\kappa} \equiv \mathbf{0}, \quad \boldsymbol{\beta}_{R/L,\kappa\kappa} \equiv \mathbf{0}, \quad \gamma_{\kappa\kappa} \equiv 0.$$

From Eqs (2.10) and (2.19) it follows that $L_{\kappa\overline{\kappa}} \equiv 0$ and the unique solubility of Eq. (2.5) therefore yields $c_{\kappa\overline{\kappa}} \equiv 0$. Eq. (2.9) and (2.18) then implies

$$(1 + L_{\kappa\kappa}*)\boldsymbol{a}_{\kappa\kappa} \equiv \mathbf{0}, \quad (1 + L_{\kappa\kappa}*)\boldsymbol{b}_{\kappa\kappa} \equiv \mathbf{0}.$$

Again the unique solubility of the resolvent equation (2.5) is used to conclude the vanishing of $\boldsymbol{a}_{\kappa\kappa}$ and $\boldsymbol{b}_{\kappa\kappa}$. Finally Eqs (2.8) and (2.17) give $\boldsymbol{\chi}_{\kappa\overline{\kappa}} \equiv \mathbf{0}$.

Conclusion 3. *If the scattering data, for three MIPs with non-parallel $\boldsymbol{k}_\parallel$, are longitudinally mirror image symmetric then the susceptibility dyadics $\boldsymbol{\chi}_{\kappa\lambda}$ have the form $\boldsymbol{\chi}_{\kappa\kappa} = \boldsymbol{\chi}_{\parallel,\kappa\kappa} + c_{\kappa\kappa}\hat{\boldsymbol{n}}\hat{\boldsymbol{n}}$ and $\boldsymbol{\chi}_{\kappa\overline{\kappa}} = \hat{\boldsymbol{n}}\boldsymbol{a}_{\kappa\overline{\kappa}} + \boldsymbol{b}_{\kappa\overline{\kappa}}\hat{\boldsymbol{n}}$.*

3.4 Axially symmetric media

Now consider a rotation around $\hat{\boldsymbol{n}}$. This rotation can be considered as an active rotation (rotate the incident directon) or a passive rotation (rotate the slab in the opposite direction). A complete set of incident directions is generated by *three* MIPs with $\boldsymbol{k}_\parallel$s mutually rotated around $\hat{\boldsymbol{n}}$, cf. Appendix A.

If the scattering data is invariant in this set the completeness of the set implies that the $\mathbf{D}_{\kappa\lambda}(\boldsymbol{k}_\parallel)$ dyadics must be axially symmetric. The uniquely determined $\boldsymbol{\alpha}_{\kappa\lambda}$,

$\boldsymbol{\beta}_{R/L,\kappa\lambda}$ and $\gamma_\kappa\lambda$ are then also axially symmetric. Hence $\boldsymbol{\beta}_{R/L,\kappa\lambda} \equiv \mathbf{0}$ which implies $\boldsymbol{a}_{\kappa\lambda} \equiv \boldsymbol{b}_{\kappa\lambda} \equiv \mathbf{0}$. cf. the transverse mirror image case. Furthermore, $\boldsymbol{\alpha}_{\kappa\lambda}$ is a linear combination of $\mathbf{I}_\parallel$ and $\mathbf{J} = \hat{\boldsymbol{n}} \times \mathbf{I}_\parallel$, since these are the only two-dimensional axially symmetric dyadics. This implies that also the dyadics $\boldsymbol{\chi}_{\parallel,\kappa\lambda}$ are linear combinations of $\mathbf{I}_\parallel$ and $\mathbf{J}$.

The susceptibility dyadics in a bianisotropic axially symmetric medium therefore take the form

$$\boldsymbol{\chi}_{\kappa\lambda} = \Psi_{\kappa\lambda}\mathbf{I}_\parallel + \Upsilon_{\kappa\lambda}\mathbf{J} + c_{\kappa\lambda}\hat{\boldsymbol{n}}\hat{\boldsymbol{n}}.$$

Moreover, the bi-isotropic media and gyrotropic non-magnetic media are contained in this class [8, 12]. However, it is not possible to detect these subclasses by using the method described in this paper. To do this the full inverse problem for a bianisotropic axially symmetric medium must be solved.

Conclusion 4. *If the scattering data, for three MIPs with mutually rotated* $\boldsymbol{k}_\parallel$*, is invariant then the susceptibility dyadics* $\boldsymbol{\chi}_{\kappa\lambda}$ *have the form* $\boldsymbol{\chi}_{\kappa\lambda} = \Psi_{\kappa\lambda}\mathbf{I}_\parallel + \Upsilon_{\kappa\lambda}\mathbf{J} + c_{\kappa\kappa}\hat{\boldsymbol{n}}\hat{\boldsymbol{n}}$*.*

3.5 Subclasses

In addition to the symmetry classes discussed in the previous subsections, subclasses can be identified. These subclasses are defined as intersections of the previously obtained symmetry classes. Define the sets

$$\begin{aligned}
\mathcal{SR} &= \{\boldsymbol{\chi}_{\kappa\lambda} \text{ such that } \boldsymbol{\chi}_{\kappa\overline{\kappa}} \equiv \mathbf{0}\},\\
\mathcal{TMI} &= \{\boldsymbol{\chi}_{\kappa\lambda} \text{ such that } \boldsymbol{\chi}_{\kappa\lambda} = \boldsymbol{\chi}_{\parallel,\kappa\lambda} + c_{\kappa\lambda}\hat{\boldsymbol{n}}\hat{\boldsymbol{n}}\},\\
\mathcal{LMI} &= \{\boldsymbol{\chi}_{\kappa\lambda} \text{ such that } \boldsymbol{\chi}_{\kappa\kappa} = \boldsymbol{\chi}_{\parallel,\kappa\kappa} + c_{\kappa\kappa}\hat{\boldsymbol{n}}\hat{\boldsymbol{n}} \text{ and } \boldsymbol{\chi}_{\kappa\overline{\kappa}} = \hat{\boldsymbol{n}}\boldsymbol{a}_{\kappa\overline{\kappa}} + \boldsymbol{b}_{\kappa\overline{\kappa}}\hat{\boldsymbol{n}}\},\\
\mathcal{A} &= \{\boldsymbol{\chi}_{\kappa\lambda} \text{ such that } \boldsymbol{\chi}_{\kappa\lambda} = \Psi_{\kappa\lambda}\mathbf{I}_\parallel + \Upsilon_{\kappa\lambda}\mathbf{J} + c_{\kappa\lambda}\hat{\boldsymbol{n}}\hat{\boldsymbol{n}}\},\\
\mathcal{MI} &= \{\boldsymbol{\chi}_{\kappa\lambda} \text{ such that } \boldsymbol{\chi}_{\kappa\kappa} = \boldsymbol{\chi}_{\parallel,\kappa\kappa} + c_{\kappa\kappa}\hat{\boldsymbol{n}}\hat{\boldsymbol{n}} \text{ and } \boldsymbol{\chi}_{\kappa\overline{\kappa}} \equiv \mathbf{0}\},\\
\mathcal{G} &= \{\boldsymbol{\chi}_{\kappa\lambda} \text{ such that } \boldsymbol{\chi}_{\kappa\kappa} = \Psi_{\kappa\kappa}\mathbf{I}_\parallel + \Upsilon_{\kappa\kappa}\mathbf{J} + c_{\kappa\kappa}\hat{\boldsymbol{n}}\hat{\boldsymbol{n}} \text{ and } \boldsymbol{\chi}_{\kappa\overline{\kappa}} \equiv \mathbf{0}\}.
\end{aligned}$$

The following relations then hold

$$\mathcal{MI} = \mathcal{SR} \cap \mathcal{TMI} = \mathcal{TMI} \cap \mathcal{LMI} = \mathcal{SR} \cap \mathcal{LMI}, \quad \mathcal{G} = \mathcal{A} \cap \mathcal{SR} = \mathcal{A} \cap \mathcal{LMI}.$$

The labels of the sets refer to the symmetry of the medium. The main symmetries are Spatial reversal ($\mathcal{SR}$), Transverse mirror image ($\mathcal{TMI}$), Longitudinal mirror image ($\mathcal{LMI}$) and Axially symmetric ($\mathcal{A}$), and the symmetries of the subclasses are denoted Mirror image ($\mathcal{MI}$) and Gyrotropic ($\mathcal{G}$). Note, $\mathcal{A} \subset \mathcal{TMI}$ implies $\mathcal{A} \cap \mathcal{TMI} = \mathcal{A}$.

4 Conclusion

By using the symmetry of the scattering data it is possible to retrieve the symmetry classes given in the previous section. Note, the incident directions can be obtained by rotating the slab and for each $\boldsymbol{k}_\parallel$ using both possible incident directions, i.e., $\hat{\boldsymbol{k}} = \boldsymbol{k}_\parallel \pm k_n \hat{\boldsymbol{n}}$.

The results can of course also be used in the direct sense, i.e., the symmetry of the scattering data can be deduced from the symmetry of the medium for any incident direction.

A reverse statement, on anisotropy, can be made by using linear constitutive relations and local spatial reversal symmetry. Consider the constitutive relations

$$\boldsymbol{D} = \mathbf{X}_{ee}(\boldsymbol{E}) + \mathbf{X}_{em}(\boldsymbol{H}), \qquad \boldsymbol{B} = \mathbf{X}_{me}(\boldsymbol{E}) + \mathbf{X}_{mm}(\boldsymbol{H}).$$

Here, each $\mathbf{X}_{\kappa\lambda}$ is a linear map, i.e., $\mathbf{X}_{\kappa\lambda}(u\boldsymbol{F} + v\boldsymbol{G}) = u\mathbf{X}_{\kappa\lambda}(\boldsymbol{F}) + v\mathbf{X}_{\kappa\lambda}(\boldsymbol{G})$. Combined use with the Maxwell equations yields

$$\begin{aligned} \nabla \times \boldsymbol{E} &= -\partial_t[\mathbf{X}_{me}(\boldsymbol{E}) + \mathbf{X}_{mm}(\boldsymbol{H})]|_{(\boldsymbol{r},t)}, \\ \nabla \times \boldsymbol{H} &= \partial_t[\mathbf{X}_{ee}(\boldsymbol{E}) + \mathbf{X}_{em}(\boldsymbol{H})]|_{(\boldsymbol{r},t)}. \end{aligned}$$

Here the fields are evaluated at $(\boldsymbol{r}, t)$. Spatial reversal or inversion corresponds to the transformations

$$\begin{aligned} \boldsymbol{E} &\to -\boldsymbol{E}, \\ \boldsymbol{H} &\to \boldsymbol{H}, \\ \nabla &\to -\nabla. \end{aligned}$$

cf. Ref. [5, p. 249], since the electric field is a vector and the magnetic field is a pseudo-vector. For a medium with local spatial reversal symmetry, the latter pair of fields also solves the combined Maxwell equations and constitutive relations. Explicitly

$$\begin{aligned} \nabla \times \boldsymbol{E} &= \partial_t[\mathbf{X}_{me}(\boldsymbol{E}) - \mathbf{X}_{mm}(\boldsymbol{H})]|_{(\boldsymbol{r},t)}, \\ \nabla \times \boldsymbol{H} &= \partial_t[\mathbf{X}_{ee}(\boldsymbol{E}) - \mathbf{X}_{em}(\boldsymbol{H})]|_{(\boldsymbol{r},t)}. \end{aligned}$$

Eliminating the left hand sides, integrating from $-\infty$ to t and assuming the fields to be quiescent at $t = -\infty$ then yields

$$\begin{aligned} \mathbf{X}_{me}(2\boldsymbol{E}) &= \mathbf{0}, \\ \mathbf{X}_{em}(2\boldsymbol{H}) &= \mathbf{0}. \end{aligned}$$

Since the fields $\boldsymbol{E}$ and $\boldsymbol{H}$ are arbitrary this implies that $\mathbf{X}_{me} \equiv \mathbf{X}_{em} \equiv \mathbf{0}$, i.e., the medium is anisotropic. Thus, local spatial reversal symmetry implies anisotropy and vice versa [9, 11].

Note, the method used in this paper does not need local spatial reversal symmetry, merely the scattering data due to a finite number of incident directions is needed. Therefore, the condition given in this paper is (much) weaker than the local condition. Due to the results of Appendix A, the condition derived in this paper is the weakest possible for homogeneous and temporal dispersive media.

The full inverse problem can also be solved by using the scattering data corresponding to three MIPs with non-parallel $\boldsymbol{k}_\parallel$. However, that problem is not adressed here.

Appendix A Complete set of incident directions

The dyadics $\mathbf{D}_{ee}\cdot\mathbf{J}$, $\mathbf{D}_{em}$, $\mathbf{J}\cdot\mathbf{D}_{me}\cdot\mathbf{J}$ and $\mathbf{J}\cdot\mathbf{D}_{mm}$, where $\mathbf{J}=\hat{\boldsymbol{n}}\times\mathbf{I}_\parallel$, are second order dyadics in $\boldsymbol{k}_\parallel$, cf. Eq. (2.20), on the form

$$\mathbf{D}(\boldsymbol{k}_\parallel)=\boldsymbol{\alpha}+\boldsymbol{k}_\parallel\boldsymbol{\beta}_R+\boldsymbol{\beta}_L\boldsymbol{k}_\parallel+\gamma\boldsymbol{k}_\parallel\boldsymbol{k}_\parallel.$$

Here $\boldsymbol{\alpha}$ is a two-dimensional dyadic normal to $\hat{\boldsymbol{n}}$, $\boldsymbol{\beta}_{L,R}$ are two-dimensional vectors normal to $\hat{\boldsymbol{n}}$ and γ is a scalar. In analogy to the scalar polynomial of second degree, $\mathbf{D}(\boldsymbol{k}_\parallel)$ is uniquely determined by *three* $\boldsymbol{k}_\parallel$s. However, these vectors must not be all parallel. To see this, take three directions $\boldsymbol{k}_\parallel=\boldsymbol{q}$ and $\boldsymbol{k}_\parallel=\boldsymbol{q}+\boldsymbol{\rho}_i$, $i=1,\,2$. Evaluation of $\mathbf{D}$ in the directions $\boldsymbol{q}+\boldsymbol{\rho}_i$ gives

$$\begin{aligned}\boldsymbol{D}(\boldsymbol{q}+\boldsymbol{\rho}_i)&=\boldsymbol{\alpha}'+\boldsymbol{\rho}_i\boldsymbol{\beta}'_R+\boldsymbol{\beta}'_L\boldsymbol{\rho}_i+\gamma\boldsymbol{\rho}_i\boldsymbol{\rho}_i,\\ \boldsymbol{\alpha}'&=\mathbf{D}(\boldsymbol{q}),\\ \boldsymbol{\beta}'_{L,R}&=\boldsymbol{\beta}_{L,R}+\gamma\boldsymbol{q}.\end{aligned}\tag{A.1}$$

Hence, the form of the dyadic $\mathbf{D}$ and the scalar parameter γ are preserved whereas $\boldsymbol{\alpha}$ and $\boldsymbol{\beta}_{L,R}$ are shifted according to Eq. (A.1). Moreover, the shifted dyadic parameter $\boldsymbol{\alpha}'$ is directly obtained as $\mathbf{D}(\boldsymbol{q})$.

The objective now is to retrieve γ and the shifted vector parameters $\boldsymbol{\beta}'_{L,R}$. To do this, introduce local polar coordinates centered at $\boldsymbol{q}$ for each i, i.e., $\boldsymbol{\rho}_i=\rho_i\hat{\boldsymbol{\rho}}_i$ and $\hat{\boldsymbol{\phi}}_i=\hat{\boldsymbol{n}}\times\hat{\boldsymbol{\rho}}_i$ $i=1,\,2$. The local polar components of $\mathbf{D}_i=\mathbf{D}(\boldsymbol{q}+\boldsymbol{\rho}_i)-\mathbf{D}(\boldsymbol{q})$ are defined as $D_i^{\rho\rho}=\hat{\boldsymbol{\rho}}_i\cdot\mathbf{D}_i\cdot\hat{\boldsymbol{\rho}}_i$, $D_i^{\phi\rho}=\hat{\boldsymbol{\phi}}_i\cdot\mathbf{D}_i\cdot\hat{\boldsymbol{\rho}}_i$ etc. Explicitly, they are

$$D_i^{\rho\rho}=\rho_i\hat{\boldsymbol{\rho}}_i\cdot(\boldsymbol{\beta}'_L+\boldsymbol{\beta}'_R)+\rho_i^2\gamma,\tag{A.2}$$

$$D_i^{\phi\rho}=\rho_i\hat{\boldsymbol{\phi}}_i\cdot\boldsymbol{\beta}'_L,\tag{A.3}$$

$$D_i^{\rho\phi}=\rho_i\hat{\boldsymbol{\phi}}_i\cdot\boldsymbol{\beta}'_R,\tag{A.4}$$

$$D_i^{\phi\phi}=0,\tag{A.5}$$

for $i=1,\,2$. Hence, the shifted vectors $\boldsymbol{\beta}'_R$ and $\boldsymbol{\beta}'_R$ can be retrieved by using Eqs (A.3) and (A.4) for $i=1,\,2$ if $\hat{\boldsymbol{n}}\cdot(\boldsymbol{\rho}_1\times\boldsymbol{\rho}_2)\neq 0$. The scalar γ is then obtained from Eq. (A.2) for either $i=1$ or 2. The other three equations in Eqs (A.2), ..., (A.5) are superfluous. Note that the number of independent components $(12-3=9)$ of

$\mathbf{D}(\boldsymbol{q})$ and $\mathbf{D}(\boldsymbol{q}+\boldsymbol{\rho}_i)$, $i = 1, 2 =$ equals the number (9) of coefficients in the parameters $\boldsymbol{\alpha}$, $\boldsymbol{\beta}_{R/L}$ and γ.

Finally, Eq. (A.1) gives the unshifted parameters since $\boldsymbol{q}$ is a known vector. Thus, the dyadic polynomial $\mathbf{D}(\boldsymbol{k}_\parallel)$ is uniquely determined by three values $\mathbf{D}(\boldsymbol{k}_\parallel^{(i)})$ if only

$$\hat{\boldsymbol{n}} \cdot [(\boldsymbol{k}_\parallel^{(1)} - \boldsymbol{k}_\parallel^{(3)}) \times (\boldsymbol{k}_\parallel^{(2)} - \boldsymbol{k}_\parallel^{(3)})] \neq 0.$$

This set of $\boldsymbol{k}_\parallel$s generates the smallest complete set of incident directions in the sense that the dyadic polynomial $\mathbf{D}(\boldsymbol{k}_\parallel)$ is uniquely determined, i.e., the exact functional form can be recovered from $\mathbf{D}(\boldsymbol{k}_\parallel^{(i)})$, $i =$, 1, 2, 3.

Appendix Acknowledgements

The author would like to thank Prof. Gerhard Kristensson at the Department of Electromagnetic Theory at Lund Institute of Technology. The work reported in this paper is supported by grants (TFR 91-849, 92-986 and 93-1145) from the Swedish Research Council for Engineering Sciences and their support is gratefully acknowledged.

References

[1] J. P. Corones, G. Kristensson, P. Nelson, and D. L. Seth, editors. *Invariant Imbedding and Inverse Problems*. SIAM, Philadelphia, 1992.

[2] J. Fridén. Inverse scattering for anisotropic mirror image symmetric media. *Inverse Problems*, **10**(5), 1133–1144, 1994.

[3] J. Fridén. Inverse scattering for the homogenous dispersive anisotropic slab using transient electromagnetic fields. Technical Report LUTEDX/(TEAT-7031)/1–23/(1994), Lund Institute of Technology, Department of Electromagnetic Theory, P.O. Box 118, S-211 00 Lund, Sweden, 1994.

[4] J. Fridén, G. Kristensson, and R. D. Stewart. Transient electromagnetic wave propagation in anisotropic dispersive media. *J. Opt. Soc. Am. A*, **10**(12), 2618–2627, 1993.

[5] J. D. Jackson. *Classical Electrodynamics*. John Wiley & Sons, New York, second edition, 1975.

[6] A. Karlsson and G. Kristensson. Constitutive relations, dissipation and reciprocity for the Maxwell equations in the time domain. *J. Electro. Waves Applic.*, **6**(5/6), 537–551, 1992.

[7] G. Kristensson and S. Rikte. The inverse scattering problem for a homogeneous bi-isotropic slab using transient data. In L. Päivärinta and E. Somersalo,

editors, *Inverse Problems in Mathematical Physics*, pages 112–125. Springer-Verlag, Berlin, 1993.

[8] G. Kristensson and S. Rikte. Transient wave propagation in reciprocal bi-isotropic media at oblique incidence. *J. Math. Phys.*, **34**(4), 1339–1359, 1993.

[9] I. V. Lindell, A. H. Sihvola, S. A. Tretyakov, and A. J. Viitanen. *Electromagnetic Waves in Chiral and Bi-isotropic Media*. Artech House, Boston, London, 1994.

[10] P. Linz. *Analytical and Numerical Methods for Volterra Equations*. SIAM, Philadelphia, 1985.

[11] T. H. O'Dell. *The Electrodynamics of Magneto-electric Media*. North-Holland, Amsterdam, 1970.

[12] H. Otterheim. *Time domain direct and inverse scattering for gyrotropic media*. PhD thesis, Royal institute of technology, Stockholm, Sweden, 1993.

Andrés Alayón Glazunov, Mats Gustafsson, Andreas F. Molisch, and Fredrik Tufvesson, "Physical Modeling of MIMO Antennas and Channels by Means of the Spherical Vector Wave Expansion,"
LUTEDX/(TEAT-7177)/1-31/(2009).

Andreas D. Ioannidis, Daniel Sjöberg, and Gerhard Kristensson, "On the propagation problem in a metallic homogeneous biisotropic waveguide,"
LUTEDX/(TEAT-7178)/1-27/(2009).

Anders Karlsson, Henrik Bladh, and Per-Erik Bengtsson, "An accurate method for predicting light scattering from soot aggregates with sub-particles of arbitrary shape and structure,"
LUTEDX/(TEAT-7179)/1-22/(2009).

Sven Nordebo, Andreas Fhager, Mats Gustafsson, Börje Nilsson, "Fisher information integral operator and spectral decomposition for inverse scattering problems,"
LUTEDX/(TEAT-7180)/1-21/(2009).

Mats Gustafsson, "Sum rule for the transmission cross section of apertures in thin opaque screens,"
LUTEDX/(TEAT-7181)/1-8/(2009).

Christer Larsson, Mats Gustafsson, and Gerhard Kristensson, "Wideband microwave measurements of the extinction cross section—Experimental techniques,"
LUTEDX/(TEAT-7182)/1-22/(2009).

Daniel Sjöberg and Mats Gustafsson, "Realization of a matching region between a radome and a ground plane,"
LUTEDX/(TEAT-7183)/1-6/(2010).

Kristin Persson, Mats Gustafsson, and Gerhard Kristensson, "Reconstruction and visualization of equivalent currents on a radome using an integral representation formulation,"
LUTEDX/(TEAT-7184)/1-45/(2010).

Mats Gustafsson, "Time-domain approach to the forward scattering sum rule,"
LUTEDX/(TEAT-7185)/1-14/(2010).

Mats Gustafsson and Daniel Sjöberg, "Sum rules and physical bounds on passive metamaterials,"
LUTEDX/(TEAT-7186)/1-19/(2010).

Mats Gustafsson, "Accurate and efficient evaluation of modal Green's functions,"
LUTEDX/(TEAT-7187)/1-10/(2010).

Alireza Kazemzadeh and Anders Karlsson, "Multilayered Wideband Absorbers for Oblique Angle of Incidence,"
LUTEDX/(TEAT-7188)/1-18/(2010).

Alireza Kazemzadeh and Anders Karlsson, "Nonmagnetic Ultra Wideband Absorber with Optimal Thickness,"
LUTEDX/(TEAT-7189)/1-14/(2010).

Daniel Sjöberg and Christer Larsson, "Cramér-Rao bounds for determination of permittivity and permeability in slabs,"
LUTEDX/(TEAT-7190)/1-13/(2010).

Anders Karlsson and Alireza Kazemzadeh, "On the Physical Limit of Radar Absorbers,"
LUTEDX/(TEAT-7191)/1-10/(2010).

Alireza Kazemzadeh, "Thin Wideband Absorber with Optimal Thickness,"
LUTEDX/(TEAT-7192)/1-9/(2010).

Anders Bernland, Annemarie Luger and Mats Gustafsson, ”Sum Rules and Constraints on Passive Systems,”
LUTEDX/(TEAT-7193)/1-28/(2010).

Anders Bernland, Mats Gustafsson, and Sven Nordebo, ”Physical Limitations on the Scattering of Electromagnetic Vector Spherical Waves,”
LUTEDX/(TEAT-7194)/1-23/(2010).

Mats Gustafsson, ”Polarizability and physical bounds on antennas in cylindrical and rectangular geometries,”
LUTEDX/(TEAT-7195)/1-11/(2010).

Christer Larsson, Daniel Sjöberg, and Lisa Elmkvist, ”Waveguide measurements of the permittivity and permeability at temperatures up to 1000 °C,”
LUTEDX/(TEAT-7196)/1-22/(2010).

Andreas Ioannidis, ”On the cavity problem for the general linear medium in Electromagnetic Theory,”
LUTEDX/(TEAT-7197)/1-13/(2010).

Mats Gustafsson and Daniel Sjöberg, ”Physical bounds and sum rules for high-impedance surfaces,”
LUTEDX/(TEAT-7198)/1-17/(2010).

Daniel Sjöberg, Mats Gustafsson, and Christer Larsson, ”Physical bounds on the all-spectrum transmission through periodic arrays: oblique incidence,”
LUTEDX/(TEAT-7199)/1-13/(2010).

Mats Gustafsson, Marius Cismasu, and Sven Nordebo, ”Absorption Efficiency and Physical Bounds on Antennas,”
LUTEDX/(TEAT-7200)/1-20/(2010).

Ruiyuan Tian, Buon Kiong Lau, and Zhinong Ying, ”Characterization of MIMO Antennas with Multiplexing Efficiency,”
LUTEDX/(TEAT-7201)/1-6/(2010).

Andreas D. Ioannidis, Gerhard Kristensson, and Ioannis G. Stratis, ”On the well-posedness of the Maxwell system for linear bianisotropic media,”
LUTEDX/(TEAT-7202)/1-25/(2010).

Gerhard Kristensson, ”The polarizability and the capacity change of a bounded object in a parallell plate capacitor,”
LUTEDX/(TEAT-7203)/1-39/(2010).